Experimental evaluation of a direct air-cooled lithium bromide-water absorption prototype for solar air conditioning

A. González-Gil, M. Izquierdo, J.D. Marcos, E. Palacios

Accepted Manuscript

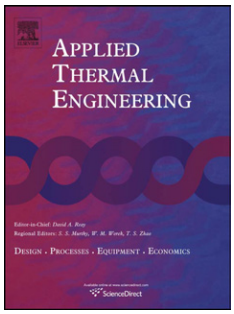

Title: Experimental evaluation of a direct air-cooled lithium bromide-water absorption prototype for solar air conditioning

Authors: A. González-Gil, M. Izquierdo, J.D. Marcos, E. Palacios

PII: S1359-4311(11)00329-2

DOI: 10.1016/j.applthermaleng.2011.06.019

Reference: ATE 3614

To appear in: *Applied Thermal Engineering*

Received Date: 2 March 2011

Revised Date: 6 May 2011

Accepted Date: 13 June 2011

Please cite this article as: A. González-Gil, M. Izquierdo, J.D. Marcos, E. Palacios. Experimental evaluation of a direct air-cooled lithium bromide-water absorption prototype for solar air conditioning, Applied Thermal Engineering (2011), doi: 10.1016/j.applthermaleng.2011.06.019

Experimental evaluation of a direct air-cooled lithium bromide-water absorption prototype for solar air conditioning

A. González-Gil [a,b,*], M. Izquierdo [a,b], J.D. Marcos [c], E. Palacios [d]

[a] Instituto de Ciencias de la Construcción Eduardo Torroja (CSIC), c/Serrano Galvache 4, 28033 Madrid, Spain
[b] Escuela Politécnica Superior, UC3M, Avenida de la Universidad 30, 28911 Leganés, Madrid, Spain
[c] Escuela Técnica Superior de Ingeniería Industrial, UNED, c/Juan del Rosal 12, 28040 Madrid, Spain,
[d] Escuela Universitaria de Ingeniería Técnica Industrial, UPM, c/Ronda de Valencia 3, 28012 Madrid, Spain
[a,b] Unidad de Asociada de Ingeniería de Sistemas Energéticos CSIC-UC3M

[*] Corresponding author: Tel./fax:+34918713248; e-mail: arturogg@ietcc.csic.es; postal address: c/Serrano Galvache 4, 28033 Madrid, Spain

ABSTRACT

A new direct air-cooled single-effect LiBr-H_2O absorption prototype is described and proposed for use in solar cooling. As distinguishing aspects, it presents: an adiabatic absorber using flat-fan sheets; an air-cooling system that directly refrigerates both the condenser and the absorber and; the possibility of being operated also as a double-effect unit. A solar facility comprising a 48 m^2 field of flat-plate collectors was used to test the single-effect operation mode of the prototype. Results from an experimental campaign carried out in Madrid during summer 2010 are shown and operation parameters corresponding to two typical summer days are detailed. The prototype worked efficiently, with COP values around 0.6. Cooling power varied from 2 kW to 3.8 kW, which represented about 85% of the prototype's nominal capacity. Chilled water temperatures mostly ranged between 14ºC and 16ºC, although the lowest measured value was of 12.8ºC. Condensation and absorption temperatures were under 50ºC and 46ºC, respectively, even with outdoor temperatures of 40ºC. Driving water temperature ranged between 85ºC and 110ºC. As a mean, the system was able to meet 65% of the cooling demand corresponding to a room of 40 m^2. No signs of crystallization were observed during about a hundred hours of operation.

Keywords: absorption, lithium bromide, direct air-cooled, solar cooling, prototype, experiment

NOMENCLATURE

A	area, m^2
COP	coefficient of performance
c_p	isobaric specific heat, kJ/kgK
I	incident solar intensity, kW/m^2
$\dot{m}$	mass flow rate, kg/s
p	pressure, kPa
PER	Primary Energy Ratio
PHE	Plate Heat Exchanger
Q	heat transfer rate, kW
R	solar radiation, kW
RTD	Resistance Temperature Detector
SCR	solar cooling ratio
SF	solar fraction
T	temperature, K
W	power consumption, kW

Greek symbols:

ε	effectiveness
η	efficiency

Subscripts:

a	absorber
ac	air cooler
aux	ancillary equipment
ca	cooling air

cf	collector field
cond	condensation
d	daily
e	evaporator/evaporation
el	electricity/electrical
g	generator
i	inlet
in	indoor
o	outlet
out	outdoor air
r	refrigerant
room	refrigerated space
s	solution
seas	seasonal
sec	secondary circuit
shx	solution heat exchanger
t	water storage tank
w	water

1. INTRODUCTION

Cooling demand is rapidly increasing in many parts of the world, especially in developed countries with moderate climates, such as most of the EU countries. This growth causes an important rise in electricity demand, being the peaks reached on hot summer days notably dangerous for the stability of electricity grids [1]. Likewise, this increasing cooling demand threatens the international agreements on CO_2 emission reduction, since consumption of fossil sources may be increased in order to meet the electricity demand. Moreover, it is necessary to add that the refrigerants commonly used in air-conditioning systems present a very high global warming potential. Even though some regulations have been approved to restrict the use of fluorinated greenhouse gases, unavoidable leakages still represents a serious problem for the environment.

Due to unsustainable situation of air-conditioning market, a great interest in solar cooling technologies emerged. The coincidence between availability of solar irradiation and peaks of cooling demand makes solar cooling a very attractive option to replace conventional refrigeration machines based on electricity. Furthermore, solar cooling systems normally use natural refrigerants, which are not harmful to the environment. Consequently, solar cooling could be considered as a suitable alternative to lower electricity consumption, to reduce dependence on fossil sources and to save greenhouse gas emissions.

Several research and demonstration projects about different solar refrigeration options have been carried out for the last years, as shown by [2], [3] or [4]. From these works, it can be extracted that, among the different technologies available for refrigeration in buildings, solar absorption cooling is the most attractive option to replace conventional electrically driven chillers. Specifically, single-effect absorption chillers using LiBr-H_2O appear to be the most interesting machines for use in solar cooling because of their simplicity and their relatively low driving temperature. However, all single-effect absorption machines currently available in the market are water-cooled. In spite of their reasonably good performance (see for instance [5] or [6], they require the installation of cooling towers to refrigerate both the condenser and the absorber. This fact makes absorption systems not only more expensive, but also less environmentally friendly because of the high water consumption, which is usually a scant source in areas with high cooling demand, such as South Europe or the Mediterranean region. In

addition to the economic perspective, cooling towers may represent a barrier to penetration of absorption chillers in the air-conditioning market because of their big size. Moreover, cooling towers are associated with growths of bacteria that may cause various diseases such as Legionella. As a result, it can be stated that small scale domestic market may not be properly covered with current absorption technology, as noticed by Ziegler some years ago [7].

Taking account of the above mentioned reasons, the development of air-cooled absorption chillers may be looked as an appropriate alternative for air-conditioning in buildings, especially in low capacity applications. This is a point also observed by other authors like Kim [8], who proposed the development of air-cooled machines as an important subject in the future R&D. However, this technology presents a major drawback, the relatively high risk of solution crystallization, due to the high working temperatures [9]. In order to overcome this difficulty, a few studies have been performed for the last years. Some of them investigated new salt mixtures that do not crystallize in such working conditions, for instance [10], [11] or [12]. Other reports analyzed new configurations for absorbers, like [13], [14], [15] or [16]. Lastly, use of lower driving temperature is seen as an alternative option to develop air-cooled LiBr-H_2O absorption chillers. In this regard, a low temperature driven absorption cycle is theoretically investigated in a recent work [17]. In this case, the cycle works with dilute LiBr-H_2O solutions to decrease risk of crystallization, but COP is about 0.37 at 35ºC ambient.

However, in spite of the numerous studies carried out, no air-cooled absorption machines are currently available on the market. Experimental results from the only air-cooled LiBr-H_2O chiller ever marketed have been reported in [18], [19] and [20]. It consisted of a single-effect absorption machine indirectly air-cooled (re-cooling) designed to work with solar energy. It was marketed by the Spanish company Rotartica until it went bankrupt a few years ago.

The “Energy Saving and Emissions Reduction in Buildings” research group, sponsored by the Eduardo Torroja Institute for Construction Science (CSIC), set out to develop new air-cooled LiBr-H_2O absorption chillers capable of competing economically with conventional compression chillers. With this aim, a new absorber-evaporator assembly permitting efficient operation at air-cooling conditions has been patented [21]. Moreover, based on that innovation, the group has recently designed, built and tested several direct air-cooled LiBr-H_2O absorption prototypes. In this context, operation details of a direct-fired double effect absorption prototype can be found in [22]. Besides, a PhD thesis comparing direct and indirect air-cooled systems for

single-effect absorption chillers was published in 2010 [23].The most recent prototype consists of a single-double-effect absorption chiller, driven by solar power (or waste heat) while operating as a single-effect apparatus or by burning fuel in the double-effect mode.

In this paper, the single-effect operation mode of the aforementioned single-double effect prototype is discussed, paying special attention to the absorber description. Additionally, the solar facility used to test this prototype is described. Results from an experimental campaign carried out in summer 2010 are shown and operation parameters corresponding to two typical summer days are detailed.

2. DESCRIPTION OF THE EXPERIMENTAL FACILITY

Figure 1 shows a schematic representation of the facility used to test the single-double effect absorption prototype in the single-effect operation mode. This facility, which has been installed in the CSIC's Experimental Plant of Solar Energy, Arganda del Rey (Madrid), essentially consists of three components, namely: solar facility, absorption prototype and chilled water distribution.

2.1. Solar facility

The solar facility designed to produce the hot water feeding the prototype's single-effect generator is formed by three different circuits. The primary circuit consists of a 48 m^2 field of evacuated flat plate solar collectors (42 m^2 useful area), a water pump and the hot side of a plat heat exchanger (PHE). The secondary circuit, designed to store the solar energy transferred from the primary circuit, includes the cold side of the PHE, a water pump and a 1500 l stratified storage tank [24]. Lastly, in the tertiary circuit a pump drives hot water from the tank to the prototype's generator. In order to avoid overheating situations, the solar facility includes a heat-dissipation system installed in the tertiary circuit. The whole solar facility is automatically controlled in order to achieve a high performance. Worth mentioning is that water pump in the secondary circuit is allowed to run only when temperature in this circuit is 2-4ºC higher than water in the storage tank. In figure 2 a picture of the solar facility is shown.

Twenty-four evacuated flat plate collectors, with 1.76 m^2 of absorber surface area each, were used in this solar facility. South-facing installed, they were arranged in four groups in such a

way that each group presented the same pressure drop. This design enables to achieve a hydraulic equilibrium and makes each collector perform at its highest. Unlike conventional flat plate collectors, in this case vacuum is maintained between the absorber surface and the collector glaze, providing a much higher insulation performance. As a result, the working fluid can reach higher temperatures. A water-glycol solution (30 wt %) was used as working fluid in the primary circuit, allowing a range of operation temperatures from -10ºC to 125ºC. By contrast, in both the secondary and tertiary circuit a concentration of 10 wt % was used since the working temperatures are not so extreme. Nominal flows corresponding to primary, secondary and tertiary circuits are, respectively, the following: 1.7 m^3/s, 1.3 m^3/s and 1 m^3/s.

2.2. Single-double-effect absorption prototype

This new prototype, designed and built by our research group, consists of a directly air-cooled LiBr-H_2O absorption chiller which can be operated as single- or double-effect. When solar energy permits to reach working temperatures, the prototype will be operated as single-effect. Otherwise, the chiller will work as a double-effect unit, being driven by energy sources such as natural gas, biofuel or even waste heat. Design cooling capacities are 4.5 kW and 7 kW, respectively.

Figure 3 shows the block diagram corresponding to the single-effect operation mode of the prototype. This configuration essentially consists of the following components: a generator, which is a PHE where the LiBr-H_2O solution is heated up to boiling by the hot water from the solar facility; a solution heat exchanger, which is also PHE, used to transfer heat from the concentrated to the diluted solution; an evaporator, which basically consists of a falling film heat exchanger to cool the water from the fancoil; a direct air-cooled adiabatic absorber (it will be described below) and; a condenser, which is a finned heat exchanger where coolant separated in the generator is directly condensed by the outdoor air. As represented in the diagram, the condensing air is previously used to cool the solution in the absorber assembly. The design of the prototype permits to use only a fan to cool both the absorber and the condenser at the same time.

Another aspect worth mentioning is that the evaporator and the absorber are assembled together in the same chamber, in such a way that the vapor generated in the evaporator is directly absorbed by the solution in the absorber. The lack of piping between these two components

significantly reduces the pressure drop and consequently improves the absorption process. Lastly, it is remarkable that all the components, except the generator, are common for both two operation modes: single- and double-effect.

The absorber assembly, which has been patented by the research group [21], transfers mass and heat separately, as an adiabatic unit. It comprises a tank to store the diluted solution, a bank of flat-fan sheet sprayers, a solution gear pump and an air-cooling system to refrigerate the solution. Through one of the sprayers, the storage tank collects concentrated solution coming from the generator. In this process, the strong solution absorbs a considerable amount of the vapor generated in the evaporator and consequently gets warmer. In order to remove this absorption heat, a solution air-cooler was assembled. As represented in figure 3, this cooling system is formed by a recirculation solution pump, a finned air heat exchanger and a fan. The diluted warmed solution is pumped through the solution-air heat exchanger (m_{sac}), where it is refrigerated directly by the outdoor air. Once cooled, it returns to the absorber storage tank through the flat-fan sheet sprayers, also contributing to the vapor absorption process. Finally, part of the solution in the tank (m_s) is pumped again to the generator completing the LiBr-H_2O solution cycle. Since the absorption process is favored by low solution temperatures, it is clearly understandable the great relevance of both the solution heat exchanger and the solution air cooler.

As stated by Palacios et al. [14], the use of flat-fan shaped sheets represents a significant improvement comparing with other absorber designs, for instance with spray absorbers [25]. This configuration increases both the mass transfer coefficient and the area available for mass transfer, significantly reducing the absorber volume. Moreover, since the flow rate is higher in sheet than in droplet sprays, absorber volume can be reduced even further. To summarize, the use of flat fan sheet sprayers affords this new generation of absorbers greater heat transfer capacity in a smaller exchange area.

2.3. Air-conditioned space and chilled water circuit.

The water chilled in the prototype's evaporator is delivered to a fan coil placed inside a laboratory's room. The space to be air-conditioned has a net floor area of 40 m^2 and a volume of 120 m^3. It is supposed to be occupied for a mean of three people from 9:00 h to 21:00 h.

Following methodology presented in [1], it is assessed that, at an outdoor temperature of 42 ºC, the thermal load for a comfortable indoor temperature of 24 ºC is about 4.5 kW.

The chilled water circuit consists of a pump and a water-air heat exchanger (fan coil) which refrigerates the space. The maximum cooling capacity of the fan coil is 7 kW. Piping is made of cooper and is properly isolated to minimize thermal loses.

3. EXPERIMENTAL APPARATUS AND PROCEDURE

The major objective of this experimental work is to test the single-effect operation mode of the above described absorption prototype. Therefore parameters of all components under different working conditions are intended to be determined.

With that aim, a measurement system was implemented on the facility. It basically consists of resistance temperature detectors (RTD), flow meters and a vacuum meter, as detailed in table 1. In Figure 3 one can roughly see the position of each sensor. RTDs were placed at the inlets and the outlets of the following components: generator (T_{iwg}, T_{owg}, T_{isg}, T_{osg}), solution heat exchanger (T_{isg}, T_{osg}, T_{isa}, T_{osa}), evaporator (T_{iwe}, T_{owe}) and solution air-cooler (T_{isac}, T_{osac}); besides, in the condenser, two RTDs measure the refrigerant condensation temperature (T_{rcond}) and the cooling-air temperature at the outlet (T_{oca}), respectively. Ultrasonic flow meters were put in the following circuits: hot water (m_{wg}), chilled water (m_{we}), diluted solution (m_s) and air-cooled solution (m_{sac}). A vacuum meter was placed inside the evaporator-absorber assembly (p_{re}). Regarding to meteorological data like solar irradiation (I) or ambient temperature (T_{out}), they were recorded by a weather station available at the Experimental Plant. Lastly, the indoor temperature corresponding to the air-conditioned space (T_{in}) is also registered by a RTD. All the measurements were made every 10 seconds and averaged every minute. A computer attached to a data acquisition system was used to register and process all the experimental data.

At this point, it is interesting to say that the utilized measurement interval is considered small enough to not miss relevant information during the prototype evaluation. As it will be shown in section 5, the variations measured in the working parameters are relatively small, mostly without steep changes. In turn, transitory regimes are also observed, mainly during the start-up and the shutdown of the prototype. However, since these transitory periods are relatively large with respect to the total experience time, the selected measurement interval is still regarded as appropriate.

The prototype was operated in such a way that the highest cooling effect could be obtained at every moment. This means that, depending on the input water temperature at the generator, the solution mass flow was regulated so that the prototype could deliver the maximum cooling power, obviously avoiding crystallization of LiBr-H_2O solution. Even though all the fluid flows in the prototype (driving hot water, chilled water, cooling air and air-cooled solution) could also be regulated, in this experimental campaign it was decided to keep them constant. It is worth mentioning that this investigation focused on testing the operation of the new prototype, although an optimization process will be performed in further works.

4. DATA REDUCTION

Although some operation parameters such as temperatures are directly measured, other important parameters have to be calculated from measurements. In the following, expressions used to obtain heat transfer rates and efficiencies are shown.

To begin with, total solar radiation on the field of collectors is calculated by

$$R_{cf} = I \cdot A_{cf} \tag{1}$$

The heat transferred from the solar collectors to the hot water storage tank is defined by

$$Q_t = \dot{m}_{w,sec} \cdot c_{p,w} \cdot (T_{iwt} - T_{awt}) \tag{2}$$

Assuming that there is not heat loss to surroundings, power delivered to LiBr-H_2O solution in the generator can be obtained as

$$Q_g = \dot{m}_{wg} \cdot c_{p,w} \cdot (T_{iwg} - T_{owg}) \tag{3}$$

Cooling capacity of the prototype can be obtained from an energy balance in the evaporator as follows

$$Q_e = \dot{m}_{w,e} \cdot c_{p,w} \cdot (T_{iwe} - T_{owe}) \tag{4}$$

Neglecting thermal losses to the surroundings, the following energy balance can be written for the chiller considered as a whole

$$Q_{ca} = Q_a + Q_{cond} = Q_e + Q_g \tag{5}$$

where the heat transferred in the absorber can be assessed by equation (6). By knowing Q_{ca} and Q_a, heat transferred in the condenser (Q_{cond}) may be obtained.

$$Q_a = \dot{m}_{sac} \cdot c_{p,s} \cdot (T_{isac} - T_{osac}) \quad (6)$$

An evaluation of the cooling effectiveness of the solution heat exchanger is made by using the following simplified equation

$$\varepsilon_{shx} = \frac{T_{osg} - T_{isa}}{T_{osg} - T_{osa}} \quad (7)$$

The thermal coefficient of performance of the prototype is obtained as the following ratio

$$COP = \frac{Q_e}{Q_g} \quad (8)$$

However, when taking into account the consumption of electricity corresponding to prototype's ancillary equipment (pumps and fan), the COP must be expressed as

$$COP_{aux} = \frac{Q_e}{Q_g + W_{aux}} \quad (9)$$

If considering the primary energy required for the production of the electricity consumed by the auxiliary equipment, prototype's performance is given by the "Primary Energy Ratio" as follows

$$PER = \frac{Q_e}{Q_g + \frac{W_{aux}}{\eta_{el}}} \quad (10)$$

where η_{el} represents the average efficiency of the electricity production process. According to the data published by the Spanish Ministry of Industry, Tourism and Trade about the electricity production in Spain [26], an average value of η_{el}=0.38 was assumed for this work.

Another parameter commonly used to measure the performance of absorption chillers is the electrical COP, which is defined as the ratio of cooling power to electrical power consumed by the prototype (equation 11)

$$COP_{el} = \frac{Q_e}{W_{aux}} \quad (11)$$

Efficiency of the whole system (including the solar facility and the absorption prototype) can be evaluated by using the solar cooling ratio (SCR), which is defined as

$$SCR = \frac{Q_e}{R_{cf}} \quad (12)$$

The average performance of the absorption prototype (daily or seasonal) is the ratio of total cooling energy production to total heat delivered to generator, as expressed by equation (13). Similarly, daily and seasonal values for COP_{aux}, PER and COP_{el} can be obtained by integrating equations (9), (10) and (11), respectively.

$$COP_{\frac{d}{seas}} = \frac{\int Q_e dt}{\int Q_g dt} \tag{13}$$

The average solar cooling system performance (daily or seasonal) is the ratio of total cooling energy production to total solar radiation on the collector field. It is expressed as

$$SCR_{\frac{d}{seas}} = \frac{\int Q_e dt}{\int R_{cf} dt} \tag{14}$$

Lastly, solar fraction (SF) gives the percentage of the total cooling demand that is met by the prototype (equation 15). Thermal load of the air-conditioned space is calculated as mentioned in section 2.3.

$$SF_{\frac{d}{seas}} = \frac{\int Q_e dt}{\int Q_{room} dt} \tag{15}$$

Needed thermodynamic properties corresponding to all the working fluids were obtained following Pátek and Klomfar [27] and ASHRAE [28].

5. EXPERIMENTAL RESULTS AND DISCUSSION

The absorption prototype was tested in single-effect operation mode during the summer of 2010. In this section, experimental results from tests carried out during two days will be detailed: 5 August and 13 July. The first day can be taken as a typical clear summer day in the region of Madrid, with maximum ambient temperatures of 35ºC. As well, it could be regarded as a representative hot summer day in other regions such as the Mediterranean coast. As regards to 13 July, it can be considered as a typical cloudless hot summer day in Madrid, with a maximum temperature of 38.5ºC. Contrary to the former day, on 13 July the experiment began before the solar radiation was high enough to power the prototype; that is, the absorption machine was started by using the heat stored in the tank during the previous day.

Finally, a summary of results corresponding to the whole experimental campaign will be presented in this section.

5.1. Results on 5 August 2010

Figure 4 shows the incident solar radiation on the field of collectors and the heat power delivered to the solar storage tank. Whereas the daily solar insolation on the collectors was 286.49 kWh, the energy transferred to the hot water in the storage tank was 52.13 kWh. The ratio between these two parameters can be regarded as the efficiency of the solar facility, which for the whole day reached a value of 0.18. However, it is notable that this efficiency presented a value of 0.32 about 14:00 h. The spikes observed around 12:00 h and 17:00 h were due to solar facility regulation. As mentioned, the pump in the secondary circuit only starts up when water temperature in this circuit is at least 2ºC higher than temperature in the storage tank. Then, several start/stop processes happened until solar irradiation was high enough to keep the solar facility working continuously (or until the facility was finally stopped).

In figure 5, temperatures corresponding to both sides of the prototype's generator are represented. At the beginning of the experiment, at 11:45 h, hot water from the solar facility entered the plate heat exchanger at 97ºC, reaching the maximum of 107ºC at 16:40 h. Although no more heat was delivered to the storage tank from about 17:20 h, the prototype continued working until 18:40 h, when temperature of hot water was 92ºC. On the other hand, LiBr-H_2O solution was heated a mean of 14ºC in the generator, ranging the outlet temperature from 80ºC to 95ºC. Spikes observed around 12:00 h and 17:00 h were mainly due to fluctuations in temperature of driving hot water, which in turn were caused by the aforementioned regulation of secondary circuit. If no heat is transferred to the storage tank, energy consumption in the prototype's generator makes hot water temperature decrease sharply. In turn, start-up of the pump in secondary circuit makes driving water temperature rise again.

Figure 5 also shows the solution temperatures at the inlet and outlet of the absorber, as well as the temperature at the outlet of the solution air-cooler. Outdoor air temperature is also represented. Note that temperatures T_{isac} and T_{osa} are exactly the same: they represent solution temperature in the absorber's tank. In the following, T_{osa} will be also referred as final absorption temperature.

As seen in figure 5, the solution air-cooler was able to reduce solution temperature about 4-5ºC, which avoided it going over 42ºC at any time. In other words, the absorber cooler made the final absorption temperature be just 5-7ºC above outdoor air temperature. This fact may be regarded as a significant achievement for development of air-cooled LiBr-H_2O absorption chillers, since the absorber is directly refrigerated by surrounding air, avoiding the secondary cooling water loop present in other air-cooled chiller designs [18]. Peaks observed in T_{isa} were mainly due to variations in input water temperature. However, it is interesting to note that two noticeable decreases in the solution mass flow contributed to make peaks between 17:00 h and 18:00 h more pronounced (see figure 7).

As regards to operation of the solution heat exchanger, it is interesting to mention that this heat plate exchanger was able to lower the temperature of solution coming from the generator up to 47 ºC under steady-state conditions. The effectiveness of the heat transfer process varied between 0.85 and 0.88 during the most of the experiment, being 0.86 the mean value. As known, the solution heat exchanger plays a key role in the absorption process, hence the interest of using an efficient heat exchanger like PHE.

Figure 6 represents the condensation temperature of the refrigerant and the cooling air temperature at the condenser outlet, after passing through the absorber cooler and the condenser. The outdoor air temperature is as well shown. It is interesting to note that the condensation temperature was maintained between 35ºC and 47ºC during the whole experiment, i.e. about 10-12ºC over the outdoor air temperature. If comparing with absorption temperature (figure 5), one can conclude that condensation temperature was about 5ºC higher.

The cooling effect of the prototype is shown in figure 6. Water temperatures at the inlet and the outlet of evaporator are represented, as well as the evaporation temperature. Besides, indoor temperature corresponding to the air-conditioned space is shown. One can see that the prototype was able to keep the indoor temperature between 23 and 25ºC by cooling down the water up to 12.8ºC. Evaporation temperature was under 10ºC for most of the time, while the minimum difference with respect to chilled water temperature was 5ºC. Whereas at the beginning of the experiment the indoor temperature was 26ºC, after an hour it was 24ºC. Likewise, the chilled water temperature went from 27ºC to 17ºC in the same period of time. The prototype can be considered to have a fast start-up time, which is regarded as an important requirement for solar cooling systems. Moreover, it is interesting to note that at the maximum

outdoor temperature (35ºC at 17:00 h) the water temperature was decreased 4.5ºC in the evaporator, reaching 13.3ºC. The lowest water temperature was 12.8ºC, measured around 16:00 h, when outdoor temperature was 33.5ºC. The slight downward slope observed in the chilled water temperature curve is due to the slightly lower increase in the cooling demand than in the prototype's cooling effect. When no more hot was supplied to the storage tank, approximately at 17:20 h, the chilled water temperature sharply increased until the end of the experiment. According to equation (15), solar fraction corresponding to this day was 100%.

Cooling capacity and input power to generator are shown in figure 7, as well as the solution mass flowing through the generator. Heat power absorbed by lithium bromide solution went from 2 kW, at the start-up, to about 5.5 kW, when the hot water temperature reached its maximum value. Whereas hot water mass flow had a constant value of 0.23 kg/s, solution mass flow varied from 0.025 kg/s to 0.055 kg/s. As seen, the input power variations are directly related to the solution mass flow regulation. When hot water temperature rises, the solution mass flow is increased. Conversely, when input water temperature goes down, the solution flow has to be diminished. The observed fluctuations in m_s could be reduced if an improved control was implemented.

On the other hand, measured cooling power ranged from 2 kW at start-up to a maximum of 3.7 kW, reached at 16.20 h. From 15:00 h to 17:15 h, when outdoor temperature varied from 32ºC to 35ºC, the cooling power stayed more or less constant around 3.5 kW, which represents about 78% of the nominal capacity. As above mentioned, the chilled water mass flow was kept constant, at a value of 0.18 kg/s. Another aspect worth mentioning is the rapid response of the prototype, which was able to deliver cooling power only 10 minutes after the start-up. Moreover, it is notable that refrigeration continued some minutes after cutting off the hot water supply. This was because of the prototype's inertia.

Figure 8 shows the total heat removed from the prototype (Q_{ca}) by the air-cooling system, as well as the heat rate transferred in the solution cooler. As explained above, the prototype's fan was operated at constant velocity, with a nominal air flow of 1.5 m^3/s. The solution mass flow through the absorber cooler was also kept constant, at a mean value of 0.47 kg/s. In the central part of the experiment, when the highest cooling effect was produced, the heat rejected to the atmosphere was about 9 kW, while the absorption heat ranged between 4 and 5 kW.

Figure 9 shows different prototype's coefficients of performance. It is seen that thermal COP values were mostly between 0.6 and 0.7. Notwithstanding in the final part of the experiment, the COP tended to rise, reaching a peak value of 0.9 around 18:00 h. This was due to the fact that, while the input heat power sharply decreased after 17:00 h, the cooling capacity decreased more slowly because of the evaporator's inertia. The spikes observed around 17:00 were mainly caused by the aforementioned regulation. The daily thermal COP presented a value of 0.65. Regarding to solar cooling ratio, it ranged between 7% and 10%, which is not far from the values obtained with water-cooled absorption chillers [6].

As far as electricity consumption by the ancillary equipment, measurements yielded a mean value of 930 W. Note that, since all the fluid flows in the prototype except for the solution mass flow were kept constant, the electric consumption stayed practically constant. Taking account of the consumption during the whole experiment, the daily performance (daily COP_{aux}) was 0.54. In turn, the daily primary energy ratio resulted to be 0.42. Lastly, the electrical COP presented a value of 2.99.

5.2. Results on 13 July 2010

In this section, the experimental results obtained on 13 July 2010 are presented. Discussion will be focused on comparing these results with those from the above exposed experiment, trying to avoid aspects that could be repetitive.

This day can be considered as a typical cloudless hot summer day in the region of Madrid, with a maximum temperature of 38.5ºC. The highest solar radiation on the collectors was 40 kW, reached around 15:00 h. During the whole day, a total solar radiation of 277.62 kWh was registered on the collector field, which is similar to the one of the previously exposed day. The energy transferred to hot water storage tank was slightly lower, 51.40 kWh. The daily efficiency of the solar facility resulted to be 0.19. However, note that at 14:00 it presented an instantaneous value of 0.32.

In figure 10 one can see that this test was started up earlier than previous, around 10:15 h. The initial water temperature was higher, about 105ºC, but in just an hour it decreased to 90 ºC. While during this period of time no heat was transferred to the storage tank, the prototype was constantly consuming energy from it. Only when solar intensity was high enough to deliver energy to the storage tank (about 600 W/m^2), the input water temperature began to increase.

The highest input water temperature, 107.7ºC, was registered at 16:30 h. Disregarding the start-up, the highest solution temperature at the outlet of the generator was 97ºC.

Data plotted in figure 11 compare temperatures measured in the absorber and the condenser with the outdoor temperature. It is interesting to note that the prototype worked properly one hour and a half after the start-up, when the input hot water reached steady conditions. Despite the fact that the input water temperature was high enough at the beginning, it suffered such a strong decrease that the control of the prototype turned out to be complex. An improved control might mitigate this problem but, in any case, it was clearly noticed that in order to successfully start up the prototype, it is necessary to have a minimum solar radiation that enables to keep hot water at adequate conditions. This is an important limitation of solar cooling systems that have been emphasized in this experiment.

In figure 11 one can see that final absorption temperature reached higher values than in the previous test, since the ambient air temperature was as well higher. The maximum value was 45.5 ºC at 17:00 h, when outdoor temperature was 38.5 ºC. During the whole experiment, final absorption temperature was kept between 5 and 8ºC over the ambient temperature. The solution heat exchanger was observed to perform at more or less the same effectiveness as in the previous exposed experiment, with a mean value of 0.86.

On the other hand, figure 11 shows that condensation temperature reached a maximum value of nearly 48ºC, while the air cooling at the outlet of the condenser was 43ºC. Again, the condensation temperature was maintained about 9-11ºC higher than the ambient air temperature at steady conditions. In spite of the higher temperatures, the air-cooling system for the condenser and the absorber performed as well as in the previous test.

Additionally, in figure 11 it is seen that the prototype was not able to produce a noticeable cooling effect until solar radiation reached the aforementioned threshold values. Only after approximately one hour and a half, the indoor temperature in the refrigerated space began to decrease continuously. It went from 29ºC, at the beginning of the experiment, to 24.5ºC, at 17:00 h. Note that from 13:30 h to 18:30 h it was under 26ºC, which is the highest comfortable temperature recommended by Spanish regulations [29]. Chilled water temperature reached its lowest value at 14:00 h, 15.8ºC. For the following three hours, it was kept more or less constant around 16ºC. Note that during this period of time, outdoor temperature varied from 34.5 to 38 ºC. After 17:00 h, hot water temperature started to decrease and, consequently, the

prototype's cooling effect became lower. About 63% of the cooling demand corresponding to this day was met by the solar system (equation 15).

Even though the input power was cut off at 18:00 h, measurement system was not turned off at this time with the aim of studying the behavior of indoor temperature without refrigeration equipment. It was clearly seen that an additional air conditioning system is needed to meet the cooling demand once the solar system is turned off. This inconvenient is regarded as one of the most important barriers to penetration of solar cooling systems in the air conditioning market. The author's proposal to efficiently supply the missing cooling power is that a fuel (fossil or renewable) powers a single-double-effect absorption chiller in the double-effect operation mode.

Data represented in figure 12 are cooling capacity and input power to prototype's generator. If neglecting the fluctuations in the beginning of the experiment, it can be seen as the prototype yielded a maximum cooling power of 3.6 kW at 14:00 h, when outdoor temperature was 35ºC. During approximately the following three hours, cooling capacity kept nearly constant around 3.3 kW, while the ambient air temperature reached 38ºC. From 17:00 h to the end of the experiment, cooling power went down because of input power decrease. Like in the previous experience, cooling effect was produced for a few minutes after cutting off the input energy due to chiller's inertia. Lastly, heat power absorbed by LiBr-H_2O solution in generator varied between 1 kW and 5.6 kW.

It is interesting to mention that the mass flow values were related to input hot water temperature in practically the same manner as in the previously exposed test. For instance, it was 0.055 kg/s when input water temperature in the generator reached 107ºC. The lowest solution mass flow measured in this experiment was 0.010 kg/s, when input water temperature was lower that 90ºC.

Figure 13 shows that, at steady conditions, the COP was around 0.62. Taking no account of the fluctuations at the beginning and the end of the experiment, the highest value for the COP was 0.76, obtained about 13:45 h. The reason of this peak in COP is that, as seen in figure 12, at that time a peak had been registered in cooling capacity, while the input power kept on increasing constantly. It is believed that an improved control system could mitigate this kind of fluctuations.

Daily COP for this day was 0.64, but in taking account of the electricity consumption (940 W as a mean) it had a value of 0.52. The daily primary energy ratio resulted to be 0.40. The solar cooling ratio, which was between 8% and 10% during most of the experiment, had a daily value of 7.3%. Lastly, the electrical COP presented a value of 2.74.

5.3. Results of the whole campaign: summary

During the present experimental campaign, which lasted from May to August, fourteen tests were carried out. It represents about 100 hours of operation under a wide range of working conditions. The prototype was driven by hot water at temperatures between 85ºC and 110ºC; the condensation temperature varied from 35ºC to 50ºC; the absorption temperature was always lower than 46ºC; the chilled water temperature ranged from 12.8ºC to 19ºC, although it was mostly between 14 and 16ºC; the cooling capacity was between 2 kW and 3.8 kW, being normally about 3-3.5 kW. It is interesting to underline that no crystallization signs were observed during the whole campaign.

Table 2 shows the energy balance of the system for each test and for the whole campaign. As seen, there is a significant scatter in the daily results, mostly caused by the different conditions under which the prototype was operated. Notwithstanding, it should be mentioned that the control system could also contribute to scatter. It has been observed that the prototype is very sensitive to flow regulation, therefore an investigation to implement a more accurate control is strongly recommended.

When making an energy balance for the whole campaign, the seasonal thermal COP presented a value of 0.59, while the EPR was 0.36. In turn the electrical COP reached a value of 2.43. However, if neglecting the three experiments where the daily thermal COP was under 0.50, the seasonal performances will be: COP= 0.63, EPR=0.38, COP_{el}=2.56.

Finally, it is interesting to mention that the experimentally obtained results were in quite good agreement with the expected results [31]. Whereas working temperatures were slightly lower than predicted, the COP presented values very similar to the simulation results.

5.4 Experimental uncertainties

Following information given in section 3 about the measurement system and according to Kline and McClintock [30], an experimental uncertainty analysis was performed. The mean results for the main parameters used in this study are shown in table 3.

6. CONCLUSIONS

A new air-cooled single-effect LiBr-H_2O absorption prototype using a flat-fan sheets adiabatic absorber is described in the present work. Unlike other air-cooled absorption chillers, in this case both the absorber and the condenser are directly cooled by the outdoor air. Another distinguishing characteristic of this chiller is that it can be operated as a double-effect unit as well. A solar facility with flat-plate collectors was used to test the single-effect operation mode of the absorption prototype under a wide range of working conditions during the summer of 2010. From the experimental results, the following conclusions were drawn:

The prototype has been working in a quite efficient way, with daily thermal COP values around 0.6 (0.38 if referred to primary energy). Cooling capacity varied from 2 kW to 3.8 kW, while the chilled water temperature reached a minimum of 12.8ºC. Condensation and absorption temperatures were always lower than 50 and 46ºC, respectively, even with outdoor temperatures of 40ºC. Driven water temperature ranged between 85ºC and 110ºC.

The prototype needed at least 93ºC to have a successful start-up. However, it was observed that when finishing experiments, the prototype could be operated at lower temperatures, normally up to 85ºC. This fact seems to be caused by thermal inertia of the prototype, but more experiments are needed to obtain a final conclusion about this issue.

After about a hundred hours of operation, no solution crystallization was noticed. This proves the feasibility of direct air-cooled single-effect LiBr-H_2O absorption chillers for solar air-conditioning applications.

Even though the system was able to meet 100% of the daily cooling demand in a few days, 35% of the seasonal cooling demand was not covered. This means that an additional air-conditioning system was needed to supply the missing cooling energy. This is a common drawback of solar cooling systems that have to be overcome so that they can compete with conventional refrigeration systems based on electricity. The author's proposal is to put single-

and double-effect operation modes together in the same absorption chiller. Thus, when solar supply is not enough to run the chiller, it can be operated as a double effect unit powered by a fossil or renewable fuel. In that way, a high performance may be obtained.

In spite of the promising results achieved with this work, it is necessary to say that the prototype is not optimized yet. The authors think that a better performance and a higher cooling capacity may be obtained, especially by implementing a more accurate regulation system. Besides, further work must be performed to reduce electricity consumption associated to ancillary equipment.

ACKNOWLEDGEMENTS

This research work was subsidized by the Spanish Ministry of Science and Innovation under research projects PSE INVISO (sub-project SP3) and ENE2010-20650-CO2-01. The authors wish to thank Emilio Martín, R&D technician, for his willing and enthusiastic contribution to the study. A. Gonzalez-Gil would like to thank CSIC for the financial support of his PhD.

REFERENCES

[1] M. Izquierdo, A. Moreno-Rodríguez, A. González-Gil, N. García-Hernando, Air conditioning in the region of Madrid, Spain: an approach to electricity consumption, economics and CO_2 emissions, Energy, in press.

[2] C.A. Balaras, G. Grossman, H.M. Henning, C.A. Infante Ferreira, E. Podesser, L. Wang, E. Wiemke, Solar air conditioning in Europe-an overview, Renew. Sust. Energ. Rev. 11 (2007) 299-314.

[3] H.M. Henning, Solar assisted air conditioning of buildings-an overview, Appl. Therm. Eng. 27 (2007) 1734-1749.

[4] K.F. Fong, T.T. Chow, C.K. Lee, Z. Lin, L.S. Chan, Comparative study of different solar cooling systems for buildings in subtropical city, Sol. Energy 84 (2010) 227-244.

[5] F. Asdrubali, S. Grignaffini, Experimental evaluation of the performances of a H_2O-LiBr absorption refrigerator under different service conditions, Int. J. Refrig. 25 (2005) 489-497.

[6] A. Syed, M. Izquierdo, P. Rodríguez, G. Maidment, J. Missenden, A. Lecuona, R. Tozer, A novel experimental investigation of a solar cooling system in Madrid, Int. J. Refrig. 28 (2005) 859-871.

[7] F. Ziegler, State of the art in sorption heat pumping and cooling technologies, Int. J. Refrig. 25 (2002) 450-459.

[8] D.S. Kim, C.A. Infante Ferreira, Solar refrigeration options-a state-of-the-art review, Int. J. Refrig. 31 (2008) 3-15.

[9] M. Izquierdo, M. Venegas, P. Rodríguez, A. Lecuona, Crystallization as a limit to develop solar air-cooled LiBr-H_2O absorption systems using low-grade heat, Sol. Energ. Mat. Sol. C. 81 (2004) 205-216.

[10] J.S. Kim, Y. Park, H. Lee, Performance evaluation of absorption chiller using LiBr+$H_2N(CH_2)_2OH$+H_2O, LiBr+$HO(CH_2)_3OH$+H_2O, and LiBr+$(HOCH_2CH_2)_2NH$+H_2O as working fluids, Appl. Therm. Eng. 19 (1999) 217-225.

[11] M. Bourouis, M. Vallès, M. Medrano, A. Coronas, Absorption of water vapour in the falling film of water-(LiBr+LiI+$LiNO_3$+LiCl) in a vertical tube at air-cooling thermal conditions, Int. J. Therm. Sci. 44 (2005) 491-498.

[12] S. Jian, F. Lin, Z. Shigang, Performance calculation of single effect absorption heat pump using LiBr + $LiNO_3$ + H_2O as working fluid, Appl. Therm. Eng. 30 (2010) 2680-2684.

[13] M. Medrano, M. Bourouis, A. Coronas, Absorption of water vapour in the falling film of water-lithium bromide inside a vertical tube at air-cooling thermal conditions, Int. J. Therm. Sci. 41 (2002) 891-898.

[14] E. Palacios, M. Izquierdo, J.D. Marcos, R. Lizarte, Evaluation of mass absorption in LiBr flat-fan sheets, Appl. Energ. 86 (2009) 2574-2582.

[15] E. Palacios, M. Izquierdo, R. Lizarte, J.D. Marcos, Lithium-bromide absorption machines: Pressure drop and mass transfer in solutions conical sheets, Energ. Convers. Manage. 50 (2009) 1802-1809.

[16] G. Xie, G Sheng, P.K. Bansal, G. Li, Absorber performance of a water/lithium-bromide absorption chiller, App. Therm. Eng. 28 (2008) 1557-1562.

[17] D.S. Kim, C.A. Infante Ferreira, Air-cooled LiBr-water absorption chillers for solar air conditioning in extremely hot weathers, Energ. Convers. Manage. 50 (2009) 1018-1025.

[18] M. Izquierdo, R. Lizarte, J.D. Marcos, G. Gutiérrez, Air conditioning using an air-cooled single effect lithium bromide absorption chiller: Results of a trial conducted in Madrid in August 2005, Appl. Therm. Eng. 28 (2008) 1074-1081.

[19] F. Agyenim, I. Knight, M. Rhodes, Design and experimental testing of the performance of an outdoor LiBr/H_2O solar thermal absorption cooling system with a cold store, Sol. Energy 84 (2010) 735-744.

[20] C. Monné, S. Alonso, F. Palacín, L. Serra, Monitoring and simulation of an existing solar powered absorption cooling system in Zaragoza (Spain), Appl. Therm. Eng. 31 (2011) 28-35.

[21] M. Izquierdo, E. Martín, E. Palacios, Absorber and absorber-evaporator assembly for absorption machines and lithium bromide-water absorption machines that integrate said absorber and absorber-evaporator assembly, Patent PCT WO2010/000571A2 and European

Patent EP2133636A1 (extended to USA, Japan, China, Canada, Brazil, Argentina, Venezuela).

[22] J.D. Marcos, Prototipo de máquina frigorífica de absorción de LiBr/H_2O de doble efecto condensada por aire, PhD thesis, Universidad Carlos III de Madrid, 2008.

[23] R. Lizarte, Evaluación experimental de máquinas de absorción de simple efecto de LiBr-H_2O de pequeña potencia condensadas por aire: sistema re-cooling frente a sistema directo, PhD thesis, Universidad Carlos III de Madrid, 2010.

[24] E. Palacios, D.M. Admiraal, J.D. Marcos, M. Izquierdo, Experimental analysis of solar thermal storage in a water tank with open side inlets, Submitted to Appl. Energ on 24 February 2011.

[25] F.S.K. Warnakulasuriya, W.M. Worek, Drop formation of swirl-jet nozzles with high viscous solution in vacuum-new absorbent in spray absorption refrigeration, Int. J. Heat Mass Transfer 51 (2008) 3362-3368.

[26] Ministerio de Industria, Comercio y Turismo (MICYT), La Energía en España 2009, MICTYT, 2010.

[27] J. Pátek, J. Klomfar, A computationally effective formulation of the thermodynamic properties of LiBr-H_2O solutions from 273 to 500 K over full composition range, Int. J. Refrig. 29 (2006) 566-578.

[28] ASHRAE Handbook – Fundamentals (SI), 2009

[29] Ministerio de Industria, Comercio y Turismo (MICYT), Reglamento de Instalaciones Térmicas en Edificios (RITE), MICYT, 2007

[30] S.J. Kline, F.A. McClintock, Describing uncertainties in single-sample experiments, Mech. Eng. 75 (1953) 3-8.

[31] J.D. Marcos, M. Izquierdo, E. Palacios, New method for COP optimization in water- and air-cooled single and double effect LiBr-water absorption machines, Int. J. Refrig.(2011), in press (doi:10.1016/j.ijrefrig.2011.03.017).

LIST OF FIGURES

LIST OF TABLES

Highlights

A novel direct air-cooled single-effect absorption prototype is described.

Feasibility of air-cooled technology for LiBr-H_2O absorption cooling is proved.

An adiabatic absorber using flat-fan sheets avoids crystallization of the solution.

A field of flat-plate collectors powers the chiller at temperatures from 85 to 110ºC.

The prototype works with thermal COP about 0.6.

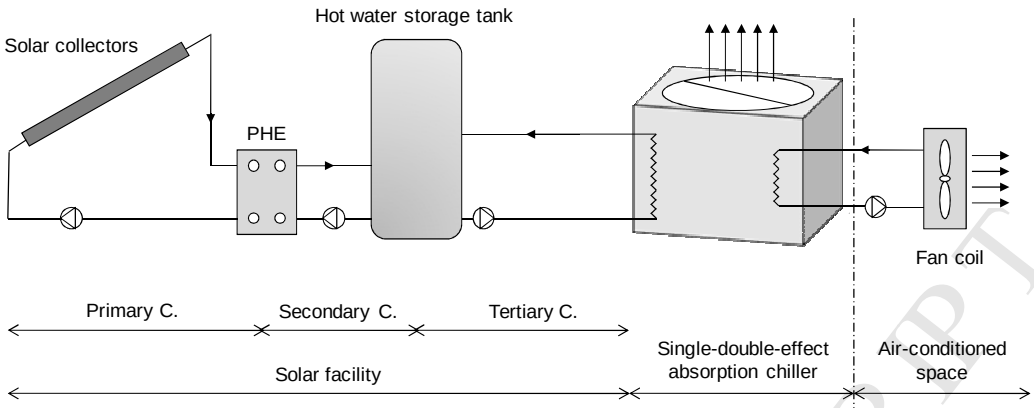

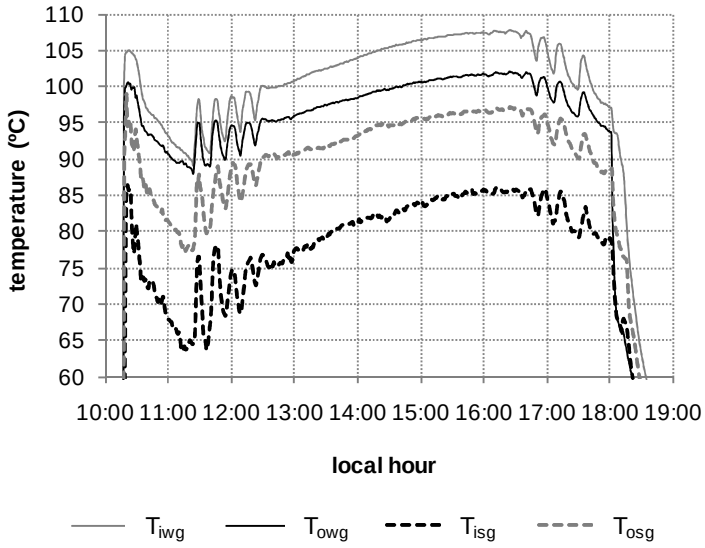

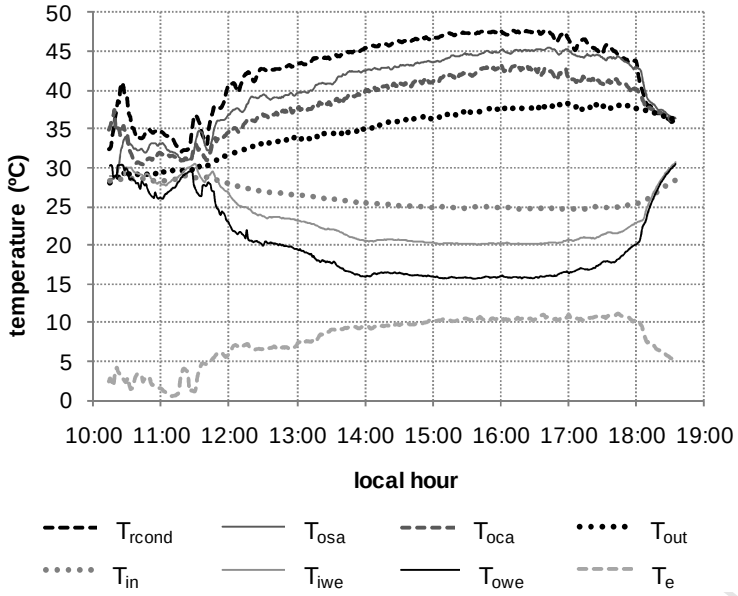

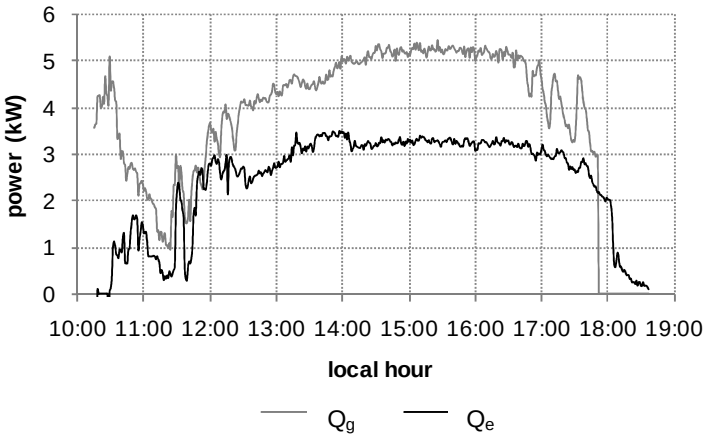

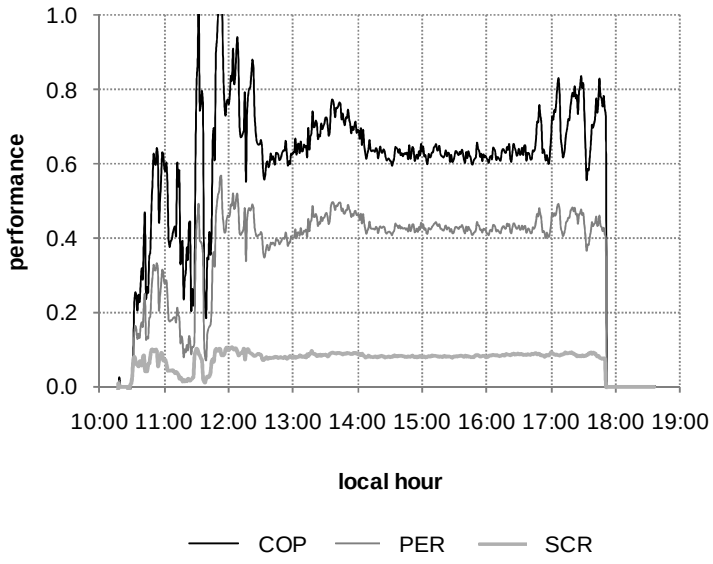

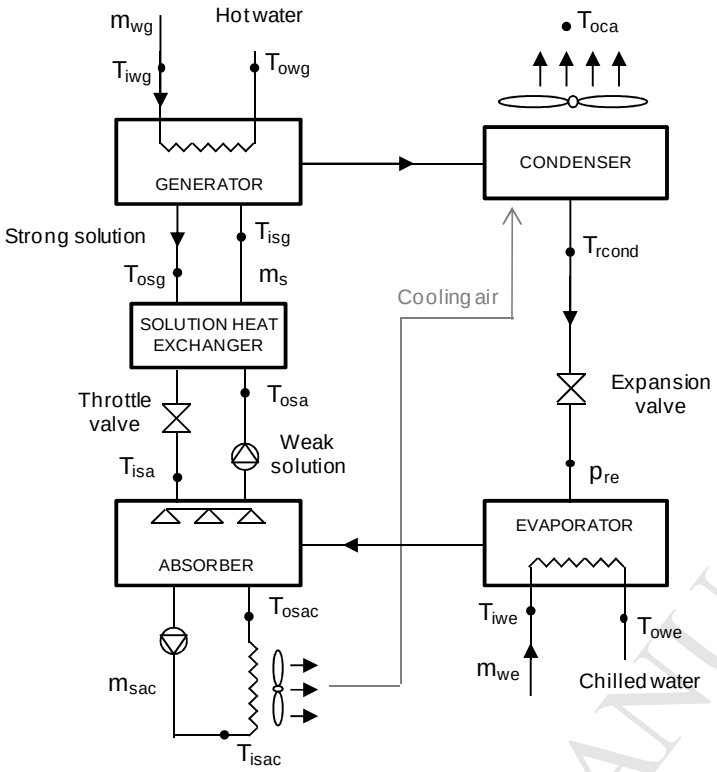

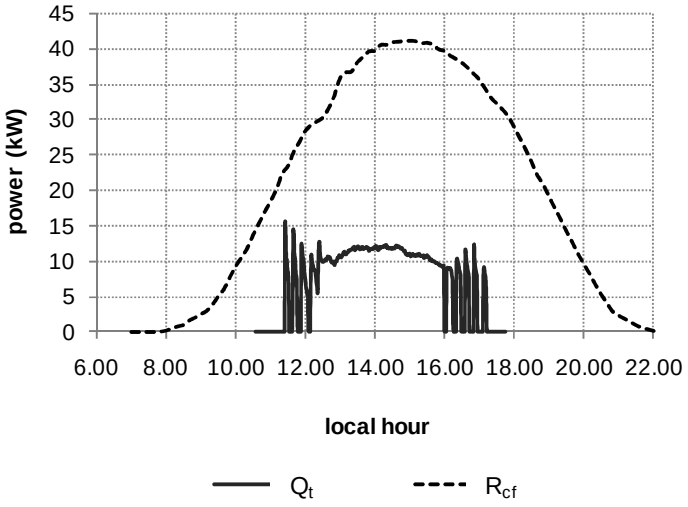

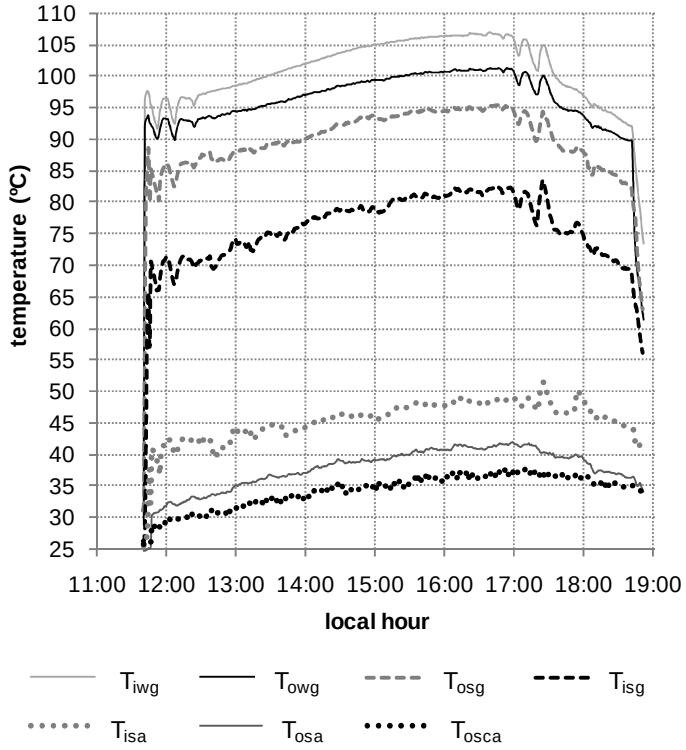

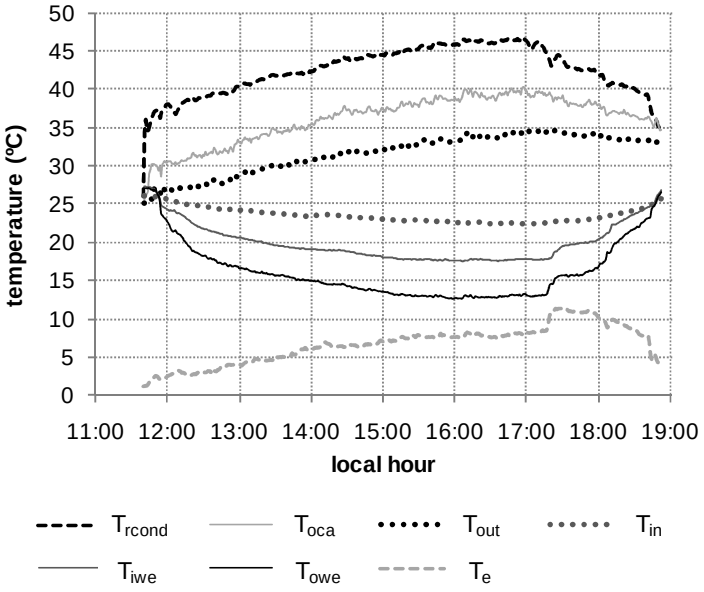

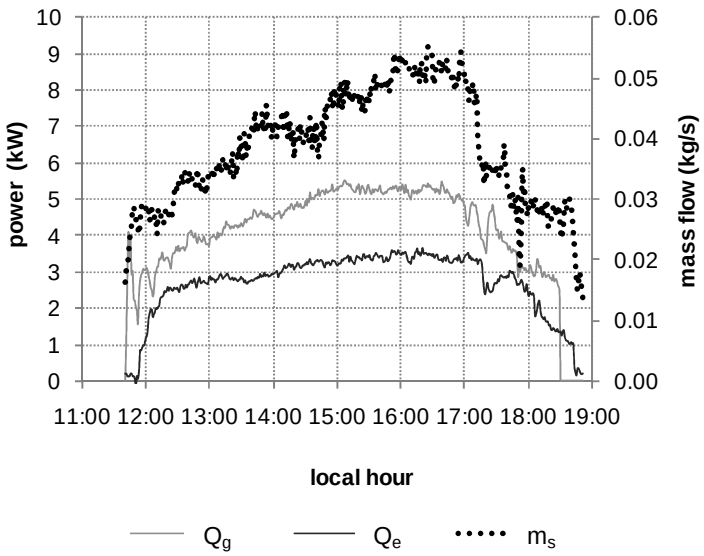

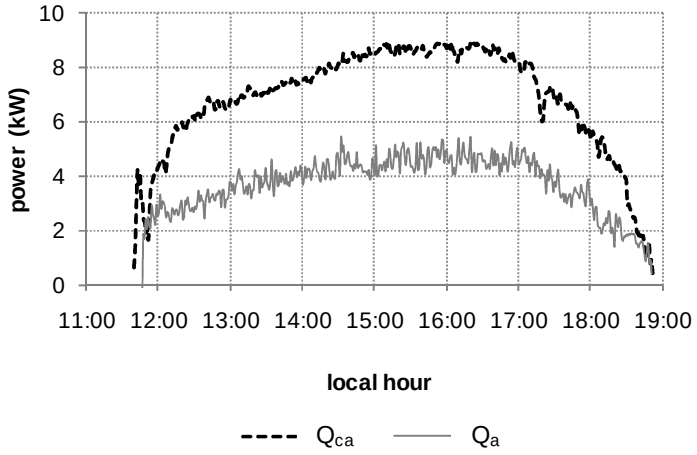

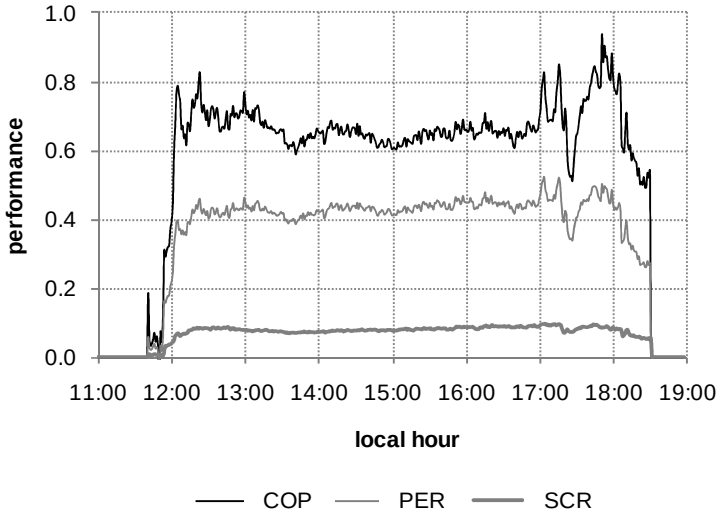

Device	Type	Range	Uncertainty
Thermometer	Pt-100 RTD	-200 to 200 ºC	±0.1 K
Flow meter	Ultrasonic	100 to 5000 l/h	1-3 %
Vacuum meter	Capacitive absolute pressure sensor	0.1 to100 mbar	0.2 % f.s

Day	Duration (h)	Daily R_{cf} (kWh)	Daily Q_t (kWh)	Daily Q_g (kWh)	Daily Q_e (kWh)	Daily COP	Daily PER	Daily COP_{el}	SF (%)
20/05/10	6.0	297.29	39.06	25.06	16.42	0.66	0.41	2.94	0.80
25/05/10	7.0	256.97	30.89	23.07	10.83	0.47	0.27	1.66	0.91
07/06/10	8.0	268.12	55.85	22.38	14.80	0.66	0.35	1.99	0.64
08/06/10	7.0	241.99	37.64	23.15	15.29	0.66	0.38	2.35	1.00
22/06/10	8.0	276.59	54.27	34.12	22.56	0.66	0.42	3.03	0.63
23/06/10	8.0	275.22	54.47	33.05	21.88	0.66	0.42	2.94	0.72
24/06/10	8.0	264.69	52.45	32.68	20.55	0.63	0.39	2.76	0.65
30/06/10	7.0	270.16	50.62	27.72	16.90	0.61	0.38	2.60	0.59
01/07/10	6.5	252.64	46.45	26.65	12.37	0.46	0.29	2.05	0.49
07/07/10	8.0	262.63	48.87	22.31	12.80	0.57	0.31	1.72	0.35
13/07/10	8.0	277.62	51.40	32.02	20.39	0.64	0.40	2.74	0.63
04/08/10	6.5	276.88	50.60	32.73	12.53	0.38	0.26	2.07	0.53
05/08/10	7.0	286.49	54.15	29.87	19.47	0.65	0.41	2.99	1.00
26/08/10	7.0	270.42	41.18	25.32	14.06	0.56	0.33	2.16	0.40
Campaign	102.0	3777.71	667.90	390.13	230.85	0.59	0.36	2.43	0.65

Operation parameter	Uncertainty
Q_t	± 2.8 %
Q_a	± 5.3 %
Q_g	± 4.0 %
Q_e	± 5.1 %
COP	± 7.6 %